

Magnetic orders of LaTiO_3 under epitaxial strain: a first-principles study

Yakui Weng,¹ Xin Huang,¹ Yankun Tang,¹ and Shuai Dong^{1, a)}
Department of Physics, Southeast University, Nanjing 211189, China

(Dated: 6 August 2018)

Perovskite LaTiO_3 bulk is a typical Mott-insulator with G-type antiferromagnetic order. In this work, the biaxial strain effects on the ground magnetic order of LaTiO_3 films grown on various substrates have been studied. For the compressive strain, LaTiO_3 films grown on LaAlO_3 , LaGaO_3 , and SrTiO_3 substrates undergo a phase transition from the original G-type antiferromagnet to A-type antiferromagnet. The underlying physical mechanisms are the lattice distortions tuned by strain. While for the tensile strain, the BaTiO_3 and LaScO_3 substrates have been tested, which show a tendency to transit the LaTiO_3 to the C-type antiferromagnet. Furthermore, our calculations find that the magnetic transitions under epitaxial strain do not change the insulating fact of LaTiO_3 .

Perovskite oxides ABO_3 have attracted continuing attention and been intensively investigated due to their novel physical properties and a broad range of technical applications.¹ Among abundant perovskite compounds, the canonical Mott insulator RTiO_3 (R^{3+} denotes a rare-earth ions) are physically interesting due to the complex couplings between the orbital, spin, lattice degrees of freedom of Ti's 3d electron which is localized by the strong Coulombic interaction. In RTiO_3 perovskites, the ligand crystal field from the oxygen octahedron splits the 5-fold 3d levels into two groups: the 3-fold t_{2g} orbitals and the 2-fold e_g orbitals. The Fermi level is located in the t_{2g} levels, and the t_{2g} orbitals are highly localized due to the $p-d$ hybridization. Moreover, the GdFeO_3 -type structure distortions, which combine the tilts and rotations of the oxygen octahedrons, are prominent in the orthorhombic RTiO_3 . According to previous studies,²⁻⁴ the ground magnetic phase of RTiO_3 transits from the ferromagnetism to G-type antiferromagnetism, with increasing size of R , or in other words with weakening GdFeO_3 -type distortions,⁵ as shown in Fig. 1(a).

In the RTiO_3 bulks, compounds with small GdFeO_3 -type distortions exhibit the G-type antiferromagnetic (AFM) ordering, e.g. LaTiO_3 , and the large ones tend to lead the FM ordering, e.g. YTiO_3 . In addition, it is well known that perovskite oxides may be sensitive to external factors.⁶⁻⁸ For example, recently the use of epitaxial strain has attracted great attentions due to many unexpected effects on thin films,⁸⁻¹² which has been proved to be a useful route to design potential devices.

In this work, the effects of epitaxial strain on the ground magnetic order of LaTiO_3 films will be studied using the first-principles calculations, as illustrated in Fig. 1(b). Our calculations predict that a robust A-type AFM phase can be stabilized by the compressive strain. In contrast, LaTiO_3 films remain G-type AFM under moderate tensile strain, but have a tendency to become the C-type AFM with further increasing the tensile strain.

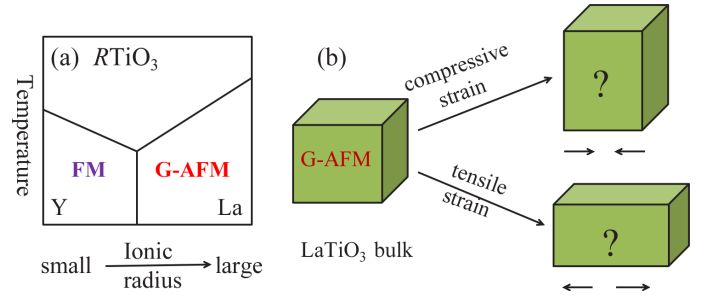


FIG. 1. (a) Sketch of experimental magnetic phase diagram of RTiO_3 . (b) Sketch of our motivation: LaTiO_3 films grown on various substrates under compressive or tensile strain.

LaTiO_3 has the orthorhombic structure (space group $Pbnm$)^{9,13} with the experimental lattice constants of $a=5.636 \text{ \AA}$, $b=5.618 \text{ \AA}$, and $c=7.916 \text{ \AA}$, containing 4 formula units.¹⁴ In the following, two different strain have been considered: in-plane compressive vs tensile. Five widely used substrates have been tested, including LaAlO_3 ($\sqrt{2}a=\sqrt{2}b=5.366 \text{ \AA}$), LaGaO_3 ($a = 5.49 \text{ \AA}$, $b=5.53 \text{ \AA}$), SrTiO_3 ($\sqrt{2}a=\sqrt{2}b=5.523 \text{ \AA}$) for the compressive case and BaTiO_3 ($\sqrt{2}a=\sqrt{2}b=5.65 \text{ \AA}$), LaScO_3 ($a=5.678 \text{ \AA}$, $b=5.787 \text{ \AA}$) for the tensile case. Here LaTiO_3 is assumed to be grown along the most studied (001) direction. Our first-principles density-functional theory (DFT) calculations are performed using the local density approximation (LDA) method with the Hubbard U and the projector-augmented wave (PAW) potentials, as implemented in the Vienna ab initio Simulation Package (VASP).^{15,16} The on-site Hubbard interaction is set as $U - J = 2.3 \text{ eV}$ using the Dudarev implementation¹⁷ for the localized 3d electrons of Ti. The lattice constants are fixed to match the particular substrate. Then the lattice constant along the (001) direction and inner atomic positions are fully optimized as the Hellman-Feynman forces are converged to less than 1.0 meV/\AA . The cutoff energy of plane-wave is 500 eV and the Brillouin-zone integrations are performed with the tetrahedron method¹⁸ over a $7 \times 7 \times 5$ Monkhorst-Pack k -point¹⁹ mesh centered at Γ .

First, the ground state of bulk LaTiO_3 has been

^{a)}Electronic mail: sdong@seu.edu.cn

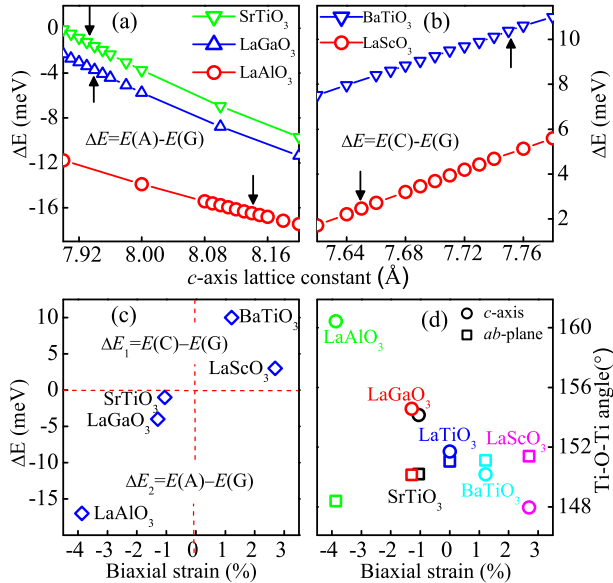


FIG. 2. (Color online) (a-b) The energy difference per Ti as a function of c lattice constant. (a) Between the A-AFM and G-AFM for the compressive cases. (b) Between the C-AFM and G-AFM for the tensile cases. (c) The energy difference (per Ti) on different substrates as a function of the biaxial strain. For the tensile strain, $\Delta E_1 = E(\text{C-AFM}) - E(\text{G-AFM})$ and for the tensile strain, $\Delta E_2 = E(\text{A-AFM}) - E(\text{G-AFM})$. (d) The Ti-O-Ti bond angles (both in-plane and out-of-plane) as a function of strain.

TABLE I. The energy difference and corresponding magnetic moment per Ti in unit of μ_B of unstrained bulk LaTiO₃: ΔE (per Ti) = $E(\text{magnetic}) - E(\text{FM})$.

Magnetic order	NM	FM	A-AFM	C-AFM	G-AFM
ΔE	124	0	-13	17	-18
Magnetic moment	0	0.86	0.80	0.77	0.75

checked. The lattice is fully optimized, giving $a=5.615$ Å, $b=5.549$ Å, and $c=7.828$ Å which are close to the experimental data. The non-magnetic (NM) state and four magnetic orders: ferromagnetic (FM), A-type AFM, C-type AFM, and G-type AFM, are calculated and compared in energy. As shown in Table I, the G-type AFM is the most stable state, as found in experiments. The calculated magnetic moment is $0.75 \mu_B$ /per Ti, slightly larger than the experimental result $0.57 \mu_B$.¹³ Our DFT calculations (Fig. 3(c)) find the insulating behavior with an energy gap of 0.45 eV, in agreement with previous DFT result⁴ and a little overestimated compared with experimental value 0.2 eV,²⁰ implying a Mott-insulator.

Subsequently, the effects of strain will be studied. For the compressive strain, the small lattice SrTiO₃, LaGaO₃, and LaAlO₃ substrates are adopted as the weak, middle, and strong cases. The internal atomic po-

sitions are relaxed with various magnetic orders within a wide range from 7.6 Å to 8.6 Å for lattice constant along the c -axis to search the optimized structure and ground state. The obtained equilibrium values for the c -axis are around 7.93 Å, 7.94 Å, and 8.14 Å for SrTiO₃, LaGaO₃, and LaAlO₃, respectively. In all these cases, the total energies show that A-type AFM is the most stable state with the relaxed structure, instead of the G-type AFM in bulk. Moreover, the FM and C-type AFM are much higher in energy than the A- and G-type AFMs. Therefore, in the following, only the results of A- and G-type AFMs will be presented for the compressive substrates.

The energy differences between these two orders are showed in Fig. 2(a). The A-type AFM is most robust (17 meV/Ti lower in energy) when grown on the LaAlO₃ substrate with the smallest in-plane lattice, while it is very fragile (only 1 meV/Ti lower in energy) on SrTiO₃. As shown in Fig. 2(c), epitaxial LaTiO₃ films on these three substrates would have a biaxial compression of about $\sim 3.8\%$ for LaAlO₃, $\sim 1.3\%$ for LaGaO₃, and $\sim 1.0\%$ for SrTiO₃, suggesting the direct relation between the magnetism and strain. In fact, our previous calculation also predicted the A-type AFM state appeared in the YTiO₃ film on the (001) LaAlO₃ substrate which is FM in bulk.²¹ The A-type AFM state does not exist in any RTiO₃ bulk so far, but may be obtained in compressive films despite the original states (FM or G-type AFM).

Next, the tensile strain effects will be studied in the same way, using BaTiO₃ and LaScO₃ as the substrates. The relaxed lattice constant along the c -axis is about 7.65 Å for LaScO₃ substrate and 7.75 Å for BaTiO₃ substrate. Different from the strain-driven phase transition in compressive cases, LaTiO₃ films remain in the G-type AFM order as in the bulk. In the tensile case, the FM and A-type AFM states have relatively higher energies than the G- and C-type AFM ones which are very proximate in energy. As shown in Fig. 2(b), with decreasing length of c -axis, the energy differences between the G- and C-type AFMs decrease, e.g. 10 meV/Ti for equilibrium length on the BaTiO₃ substrate, and 3 meV/Ti for the LaScO₃ case. These results show that the tensile LaTiO₃ films have an obvious tendency to be C-type AFM if further large lattice substrates are used. These new phases (the A-type and possible C-type AFMs) are physical interesting, which enrich the magnetic phase diagram of the RTiO₃ family.

As stated before, the Ti-O-Ti bond angles can be used as a parameter to characterize the lattice distortions in RTiO₃. As shown in Fig. 2(d), with increasing biaxial compression, the bond angles decrease in the ab -plane but increase along the c -axis, while the tensile strain gives the opposite trend. According to RTiO₃ bulk's phase diagram, the relation between lattice distortions and magnetic orders are well-established: FM order for strong distortions (small Ti-O-Ti bond angles), AFM order for weak distortions (large Ti-O-Ti bond angles). Thus, the compressive strain, which decreases the in-plane bond angles but increase the out-of-plane one, tends to make

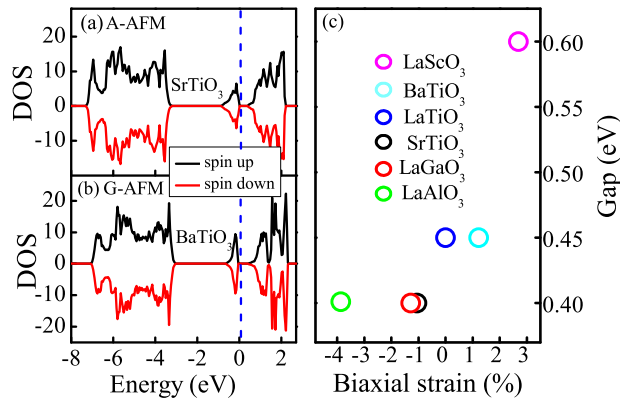


FIG. 3. (Color online) Total DOSs of LaTiO_3 films under strain. (a) on SrTiO_3 . (b) on BaTiO_3 . The Fermi energy is located in zero. (c) The energy gap as a function of strain.

spins arrange parallel in-plane and anti-parallel along the c -axis, namely the A-type AFM order. In contrast, for the tensile cases, the opposite changes of bond angles favor the AFM coupling in-plane but FM coupling along the c -axis, namely the C-type AFM tendency although it has not been achieved on BaTiO_3 and LaScO_3 substrates.

Moreover, for all strained LaTiO_3 , the insulating behavior has been preserved despite the magnetic phase transitions. For example, the DOSs of LaTiO_3 films grown on SrTiO_3 and BaTiO_3 substrates are shown in Fig. 3(a) and 3(b), respectively. In both cases, a gap exists at the Fermi level. The states near the Fermi level is dominated by Ti t_{2g} levels. The tiny difference of DOSs between the SrTiO_3 and BaTiO_3 , can also reflect the strain effect to the electronic structure. As summarized in Fig. 3(c), the band gap increases slightly from the compressive strain to tensile strain.

In conclusion, the magnetic orders of LaTiO_3 films with the biaxial compressive and tensile strain have been studied using LDA+ U method. For the compressive

strain, a phase transition from G-type AFM to A-type AFM has been found and this transition is much more robust when the strain increases. However, the G-type AFM still be the ground state for the tensile strain and the C-type AFM maybe appear if the strain is further increased. Furthermore, the LaTiO_3 films preserve the insulating behavior on all substrates studied here.

Work was supported by the 973 Projects of China (Grant No. 2011CB922101), NSFC (Grant Nos. 11274060, 51322206).

¹E. Dagotto, *Science* **309**, 257 (2005).

²M. Imada, A. Fujimori, and Y. Tokura, *Rev. Mod. Phys.* **70**, 1039 (1998).

³I. V. Solovyev, *Phys. Rev. B* **69**, 134403 (2004).

⁴S. Okatov, A. Poteryaev, and A. Lichtenstein, *EPL* **70**, 499 (2005).

⁵M. Mochizukui and M. Imada, *New J. Phys.* **6**, 154 (2004).

⁶S. Dong, S. Dai, X. Y. Yao, K. F. Wang, C. Zhu, and J.-M. Liu, *Phys. Rev. B* **73**, 104404 (2006).

⁷S. Dong, Q. F. Zhang, S. Yunoki, J.-M. Liu, and E. Dagotto, *Phys. Rev. B* **86**, 205121 (2012).

⁸E. Bousquet and P. Ghosez, *Phys. Rev. B* **74**, 180101 (2006).

⁹J. M. Rondinelli and N. A. Spaldin, *Adv. Mater.* **23**, 3363 (2011).

¹⁰D. G. Schlom, L.-Q. Chen, C.-B. Eom, K. M. Rabe, S. K. Streifler, and J.-M. Triscone, *Annu. Rev. Mater. Res.* **37**, 589 (2007).

¹¹P. Zubko, S. Gariglio, M. Gabay, P. Ghosez, and J.-M. Triscone, *Annu. Rev. Condens. Matter Phys.* **2**, 141 (2011).

¹²S. Dong, R. Yu, S. Yunoki, G. Alvarez, J.-M. Liu, and E. Dagotto, *Phys. Rev. B* **78**, 201102(R) (2008).

¹³M. Cwik, T. Lorenz, J. Baier, R. Muller, G. Andre, F. Bouree, F. Lichtenberg, A. Freimuth, R. Schmitz, E. Muller-Hartmann, and M. Braden, *Phys. Rev. B* **68**, 060401 (2003).

¹⁴A. C. Komarek, H. Roth, M. Cwik, W.-D. Stein, J. Baier, M. Kriener, F. Bourée, T. Lorenz, and M. Braden, *Phys. Rev. B* **75**, 224402 (2007).

¹⁵G. Kresse and J. Hafner, *Phys. Rev. B* **47**, 558 (1993).

¹⁶G. Kresse and J. Furthmüller, *Phys. Rev. B* **54**, 11169 (1996).

¹⁷S. L. Dudarev, G. A. Botton, S. Y. Savrasov, C. J. Humphreys, and A. P. Sutton, *Phys. Rev. B* **57**, 1505 (1998).

¹⁸P. E. Blöchl, O. Jepsen, and O. K. Andersen, *Phys. Rev. B* **49**, 16223 (1994).

¹⁹H. Monkhorst and J. D. Pack, *Phys. Rev. B* **13**, 5188 (1976).

²⁰Y. Okimoto, T. Katsufuji, T. Arima, and Y. Tokura, *Phys. Rev. B* **51**, 9581 (1995).

²¹X. Huang, Y. K. Tang, and S. Dong, *J. Appl. Phys.* **113**, 17E108 (2013).